Hydrogeol J (2016) 24:1953–1966
DOI 10.1007/s10040-016-1445-4

REPORT

A multi-tracer approach to delineate groundwater dynamics in the Rio Actopan Basin, Veracruz State, Mexico

Juan Pérez Quezadas[1] · **Victor M. Heilweil**[2] · **Alejandra Cortés Silva**[3] · **Luis Araguas**[4] · **María del Rocío Salas Ortega**[5]

Received: 17 December 2015 / Accepted: 27 June 2016 / Published online: 21 July 2016

Abstract Geochemistry and environmental tracers were used to understand groundwater resources, recharge processes, and potential sources of contamination in the Rio Actopan Basin, Veracruz State, Mexico. Total dissolved solids are lower in wells and springs located in the basin uplands compared with those closer to the coast, likely associated with rock/water interaction. Geochemical results also indicate some saltwater intrusion near the coast and increased nitrate near urban centers. Stable isotopes show that precipitation is the source of recharge to the groundwater system. Interestingly, some high-elevation springs are more isotopically enriched than average annual precipitation at higher elevations, indicating preferential recharge during the drier but cooler winter months when evapotranspiration is reduced. In contrast, groundwater below 1,200 m elevation is more isotopically depleted than average precipitation, indicating recharge occurring at much higher elevation than the sampling site. Relatively cool recharge temperatures, derived from noble gas measurements at four sites (11–20 °C), also suggest higher elevation recharge. Environmental tracers indicate that groundwater residence time in the basin ranges from 12,000 years to modern. While this large range shows varying groundwater flowpaths and travel times, ages using different tracer methods (^{14}C, $^{3}H/^{3}He$, CFCs) were generally consistent. Comparing multiple tracers such as CFC-12 with CFC-113 indicates piston-flow to some discharge points, yet binary mixing of young and older groundwater at other points. In summary, groundwater within the Rio Actopan Basin watershed is relatively young (Holocene) and the majority of recharge occurs in the basin uplands and moves towards the coast.

Keywords Groundwater flow · Radiocarbon · Noble gases · Groundwater age · Mexico

Electronic supplementary material The online version of this article (doi:10.1007/s10040-016-1445-4) contains supplementary material, which is available to authorized users.

✉ Juan Pérez Quezadas
pquezadas_1@hotmail.com

[1] Posgrado en Ciencias de la Tierra, Universidad Nacional Autónoma de México, UNAM, Campus Juriquilla, Blvd. Juriquilla No. 3001, Querétaro 76230, Mexico

[2] US Geological Survey, 2329 Orton Circle, Salt Lake City, UT 84119, USA

[3] Instituto de Geofísica, Universidad Nacional Autónoma de México, UNAM, Ciudad Universitaria, Delegación Coyoacán 04510, Mexico, D.F., Mexico

[4] Isotope Hydrology Section, International Atomic Energy Agency, Vienna International Centre, PO Box 100, 1400 Vienna, Austria

[5] Centro de Ciencias de la Tierra, Universidad Veracruzana, Francisco J. Moreno 207, Col. Emiliano Zapata, Xalapa, Veracruz, Mexico C.P. 91090

Introduction

The availability of groundwater resources for human use depends not only on the quantity and quality of water in residence at any given time, but also on the rate that water replenishes an aquifer (Healy et al. 2007). Dating of groundwater using environmental tracers can be used for both evaluating the rate at which the groundwater is replenished and to better understand flow and transport processes (Cook and Bohlke 2000). In mountainous terrain, the use of noble-gas thermometry can provide additional constraints on recharge zone elevation (Aeschbach-Hertig et al. 1999; Manning and Solomon 2003; Gardner and Heilweil 2014). Most groundwater samples from both springs and production wells with long screened intervals represent mixtures of multiple flow paths.

The combination of tracers reflecting different timescales is both a powerful and necessary approach when studying residence times of groundwater following varying pathways and having a wide range of travel times (Plummer et al. 1993; Newman at al. 2010). Combining the measurements of two or more different tracers with very different dating ranges can make the presence of such mixtures obvious by showing discrepant ages (IAEA 2013). This has been particularly useful in studies for evaluating binary mixtures of recent (<60 years) and older (>1,000 years) groundwater in fractured or karstic bedrock aquifers (Yager et al. 2013; Heilweil et al. 2014).

The Rio Actopan Basin extends over 2,000 km^2 in the central part of the Veracruz State, Mexico. The center of the basin is located 19°32′5.11″ latitude north and 96°41′39.89″ longitude west; between 2,110,000 and 2,180,000 UTM latitude N (Fig. 1). Its shape is elongated in an orientation northwest to southeast (approximately 90 km long) and narrower from northeast to southwest (approximately 20 km wide). It is bounded on the east by the Gulf of Mexico and to the west by the Sierra Madre Oriental. The topographic relief is variable and characterized by two main areas: a lower-elevation lower-gradient sector along the coast, and a higher-elevation steeper sector situated in the Sierra Madre Oriental Mountains (Tejeda et al. 1989). The altitudinal gradient is extremely large in this short distance, rising from sea level at the Port of Veracruz to 4,220 m above sea level (masl) at the peak of the extinct Cofre de Perote volcano in less than 70 km. As expected, the stable-isotope (δ^2H, $\delta^{18}O$) gradient and precipitation patterns in the study area are greatly influenced by these topographic features (Pérez Quezadas et al. 2015).

Due to the relative abundance of surface water in the Rio Actopan Basin, previous studies on groundwater dynamics and (or) water quality aspects in the study area have been limited. A CONAGUA (2002) study found that the unconsolidated alluvial aquifer located in the coastal area in the eastern part of the basin was partially recharged by the Actopan River, as indicated by observed streamflow losses at the hydrographic stations of Ídolos, Actopan and Naranjillo. A study of several springs in the vicinity of the Emiliano Zapata municipality showed that the occurrence of springs is controlled by the lithological contrast of the different geological units (Salas-Ortega 2010).

The objective of this study was to identify recharge zones, directions of groundwater flow, and groundwater ages (transit time) in the Río Actopan Basin using water chemistry and environmental tracers. Such information would provide a better understanding of the processes controlling regional groundwater occurrence, pathways, and interactions with surface water. In particular, the data collection and interpretation in this study were focused on testing the hypotheses that (1) the groundwater within the watershed is relatively young, indicating an active flow system in highly permeable aquifers driven by large hydraulic gradients; and (2) the majority of recharge to the groundwater system occurs in the upland parts of the watershed and moves towards the coast.

Study area

Climate and precipitation

The climate within the study area varies from "tropical wet-and-dry" (average annual temperature > 18 °C and more than 150 mm precipitation during the summer months) at the Port of Veracruz to "humid subtropical" (average temperature > 10 °C during the warmest months and more than 1,200 mm of rain during the wet season) in the Sierra Madre Oriental mountains (Geo-Mexico 2014). The maximum monthly air temperature occurs during May and June. Mean annual air temperature at 3,100 masl is 9.6 °C; at 1,400 masl is 18.3 °C and at sea level is 25.6 °C (Hernández López 2012). The seasonal variation of temperature at three weather stations is 4 °C at 3,000 masl, 8 °C at 1,400 masl, and 6 °C at sea level. The primary controls on the local climate within the study area are both topography and the atmospheric circulation systems prevailing during the different seasons (Mosiño and García 1973). These factors result in the occurrence of a rainy season during summer and autumn. Although the study area is located within the tropics, the precipitation regime is also affected by mid-latitude phenomena such as extratropical cyclones (Jones et al. 2003). About 80 % of total annual rainfall occurs between June and October. It is also interesting to note that the monthly amount of precipitation during the rainy season is similar for both high- and low-elevation stations (Tembladeras and Port of Veracruz, respectively). While rainfall during the months of July and August exceeds 300 mm at both these stations, precipitation during the same months at Xalapa is less than 200 mm. It is theorized that a local vertical circulation pattern caused by a barometric pressure anomaly causes a microclimate that brings drier air to the Xalapa area during the summer months (Pérez Quezadas et al. 2015).

There is also a large inter-annual variability in total rainfall within the study area. Total annual rainfall varied from 1,206 to 2,076 mm at the station in Global Network of Isotopes in Precipitation (GNIP), during 1962–1988. This station was located at coordinates 19°12′00″ latitude N and 96°07′48″ longitude west in Port of Veracruz. This variation in the precipitation is associated with global phenomena such as El Niño - Southern Oscillation (ENSO; Rasmusson and Wallace 1983), and La Niña (the negative phase), resulting in excess rain in some parts of the state of Veracruz during the summer (Magaña et al. 2003). The Pacific Decadal Oscillation (PDO; Mantua et al. 1997), in its negative phase, can also induce excessive rain in southern portion of the state of Veracruz (Méndez González et al. 2010). Lastly, the Atlantic

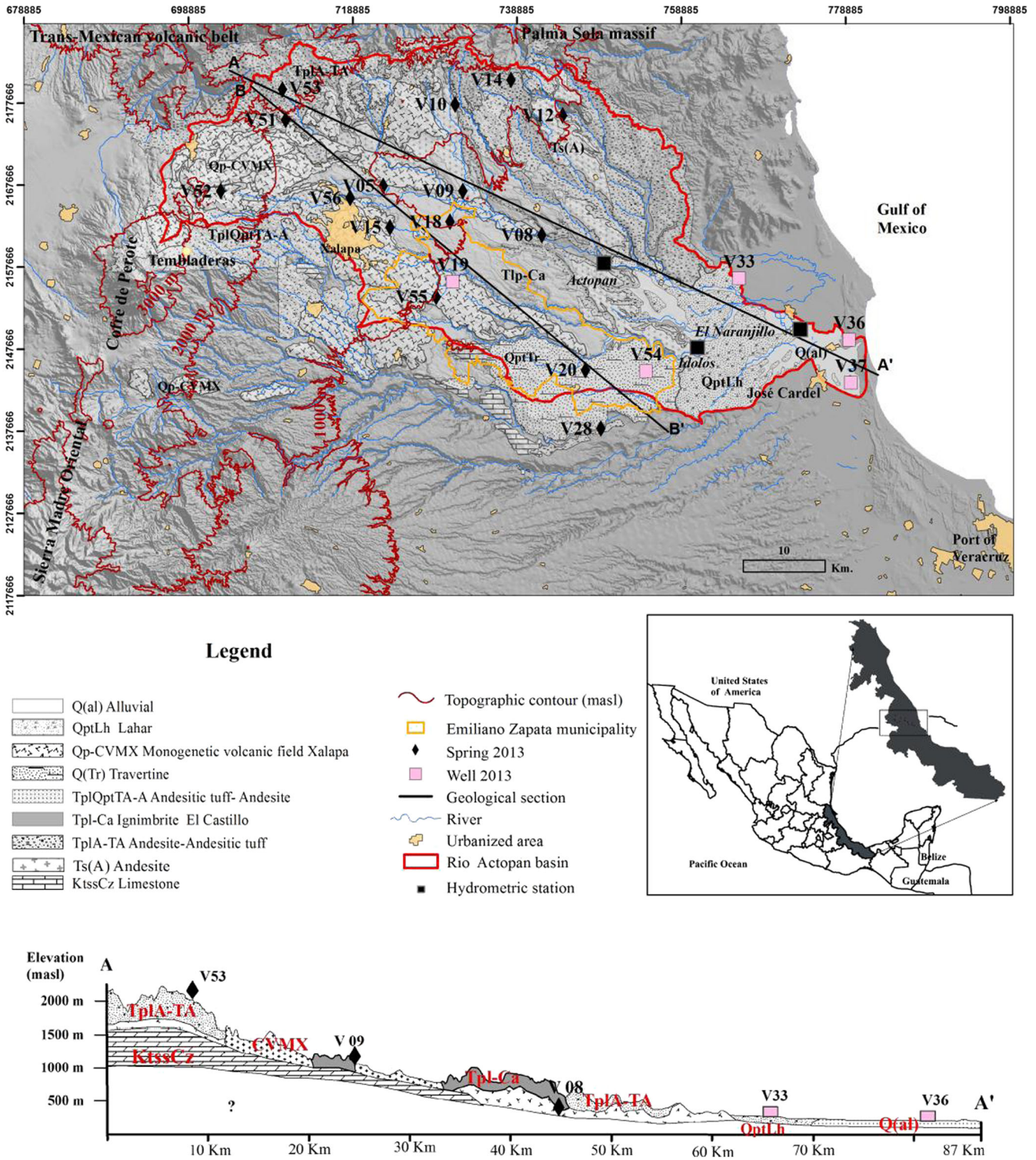

Fig. 1 Simplified geological map and cross-section (*A*–*A′*) of the Rio Actopan Basin, indicating the location of the groundwater sampling sites. Cross-section *B*–*B′* is shown in Fig. 5

Multidecadal Oscillation (AMO; Sutton and Hodson 2005) can increase the frequency of hurricanes, causing excessive rainfall in the state of Veracruz (Vázquez 2007).

Goldsmith et al. (2011) used environmental isotopes to carry out a water balance study in the tropical forest of the central part of the state of Veracruz. They found a marked

seasonality variation in the isotopic composition of precipitation of about 130 ‰ for δ^2H and 18 ‰ for $\delta^{18}O$, with more isotopically depleted precipitation during the rainy season. This observation is consistent with the historical isotope records of the Port of Veracruz GNIP station, which was operated from 1962 to 1987. Recently, Pérez Quezadas et al. (2015) found an $\delta^{18}O$ isotopic gradient in precipitation within the Rio Actopan Basin of −2.1 ‰ km^{-1} from the sea level to about 4,200 masl. That study also identified an inverse relationship between monthly precipitation amount and $\delta^{18}O$, with rainfall during the wet summer season (June–October) depleted by up to −5 ‰ compared with rainfall during the dry winter season, based on historical (1962–1988) data from the Port of Veracruz.

Geology of the Rio Actopan Basin

The geological framework of the Rio Actopan Basin has been recently delineated by the Servicio Geológico Mexicano (2007a, b; 2010). The oldest rocks cropping out in the basin are of Mesozoic and Tertiary age, overlain by alkaline volcanic rocks of the Miocene (Campo Volcánico Palma Sola), followed by volcanic rocks of the Pliocene, and the more recent Quaternary magmatic rocks of the Trans-Mexican Volcanic Belt (Fig. 1).

The pre-volcanic basement of the area is formed by limestones and other carbonate rocks of the Upper Mesozoic (Cretaceous), locally known as the Guzmantla Fm (Viniegra-Osorio 1965). These formations have been assigned to the Turonian age and were deposited in a continental platform depositional environment. In the southern part of the study area, marly rocks, lutites and carbonaceous mudstones have been reported and dated as Late Cretaceous Campanian-Maastrichtian (Servicio Geológico Mexicano 2010).

In the northern part of the basin, the dominant geological feature is Palma Sola volcanic field, which is part of the Western Alkaline Province. In this region, andesitic rocks of the middle Miocene are overlain by pyroclastic flows that have been dated by Negendank et al. (1985) and López-Infanzón (1991) as Miocene. The northwestern part of the basin is dominated by upper Pliocene to early Pleistocene andesite and andesitic tuffs. Outcrops of these andesitic tuffs have a typical thickness of several tens of meters and are located at elevations ranging from 1,000 to 3,000 masl. In the center of the basin, (northeast of the city of Xalapa) there are outcrops of late Pliocene rhyolitic ignimbrite (Morales-Barrera 2009). This is overlain by Pliocene and Pleistocene andesitic-andesite tuffs, which outcrop further north.

A major feature of the Quaternary deposits in the Rio Actopan Basin is an extensive formation of massive, recrystallized Pleistocene travertine. This formation is discordantly positioned over the Cretaceous limestones. In the west and central parts of the basin, the most prominent and geologically recent feature is the monogenetic volcanic field of Xalapa, which is formed by 59 volcanic structures extending over 2,400 km^2 (Fig. 1). Holocene alluvial deposits and colluvial sediments along the main river channels are the most recent formations in the basin (Rodríguez et al. 2010).

Hydrogeological setting

Synthesizing published geological information, five main hydrogeologic units are proposed for the Rio Actopan Basin groundwater system: (1) Quaternary alluvial deposits up to about 300 m in thickness (CONAGUA 2002), (2) Quaternary volcanics (including the volcanic field of Xalapa, with variable thickness up to tens of meters; Rodríguez et al. 2010), (3) Pliocene ignimbrites about 80 m in thickness (Morales-Barrera 2009), (4) Pliocene and Pleistocene andesitic tuffs and andesites up to about 500 m in thickness (Gómez 2002), and (5) a unit composed of both Pleistocene travertine (several meters in thickness) and Cretaceous limestone (more than 500 m in thickness; Santamaría-Orozco et al. 1990).

Most groundwater extraction occurs in the coastal area, usually from wells with total depths less than 150 m. These high-yielding wells are screened in the unconfined Quaternary alluvial aquifer comprised of gravels and sands; nearest the coast, these deposits also contain clays. The transmissivity of this unit ranges from 1 to 95×10^{-3} m^2/s (CONAGUA 2002). In contrast to wells located primarily at lower elevations, most of the spring discharge emanates higher up in the basin from the Quaternary volcanics, which have high permeability resulting from both fractures and lava-flow structures. These springs have flow rates of up to several m^3/s. In the center of the basin, especially in areas with abundant andesitic tuffs, some springs likely discharge from perched aquifers. The Pliocene ignimbrites are less fractured, resulting in springs with smaller flow rates, often less than 5 L/s. The deepest well in the basin (V29, 200 m depth) is located in this formation. No springs with significant flow rates have been identified in the areas dominated by the Pliocene and Pleistocene andesitic formations. Major springs V28 and V20 (discharging up to 1 m^3/s), along with well V54, are located in the combined Pleistocene travertine and Cretaceous limestone formations (Table 1). The limestone has differing amounts of karstification, caused by variable fracturing and dissolution features.

Major tectonic structures (fault lineaments) within the Rio Actopan Basin are aligned along the SE–NW direction (Fig. 2). Many springs are located either along these structures or in areas of steep hydraulic gradients, usually discharging into rivers and streams. In some cases, major springs are

Table 1 Site information for groundwater sampling during 2013 in the Rio Actopan Basin, Veracruz, Mexico. Analysis Types: *C/I* indicates chemistry and stable isotope (δ^2H, δ^{18}O) results presented in Table S1 of the ESM; *T/C* indicates tritium (^{3}H) and carbon isotope (^{14}C, δ^{13}C) results presented in Table S2 of the ESM; *CFC* indicates CFC-11, CFC-12, and CFC-113 results also presented in Table S2 of the ESM; *NG* indicates noble gas (He, Ne, Ar, Kr, Xe) results presented in Table S3 of the ESM

Site No.	Site type	Site name	Hydrogeologic unit of discharge	Date (dd/mm/yyyy)	Latitude	Longitude	Elevation (masl)	Analysis types
V05	Spring	Paso de San Juan	Pliocene Ignimbrites	05/07/2013	19°35′ 27.0″	96°52′ 39.9″	950	C/I, T/C
V08	Spring	El Descabezadero	Quaternary Volcanics	04/25/2013	19°32′ 04.4″	96°41′ 40.4″	366	C/I, T/C, CFC
V09	Spring	El Nacimiento Almolonga	Quaternary Volcanics	04/23/2013	19°35′ 02.0″	96°47′ 08.0″	822	C/I, T/C, CFC, NG
V10	Spring	Tepetlan	Pliocene/Pleistocene Andesite-Andesite Tuff	05/07/2013	19°40′ 45.9″	96°47′ 34.7″	1,246	C/I
V12	Spring	Topiltepec	Pliocene/Pleistocene Andesite-Andesite Tuff	05/08/2013	19°39′ 56.8″	96°40′ 05.7″	700	C/I
V14	Spring	La Cañada Xomotla	Pliocene/Pleistocene Andesite-Andesite Tuff	05/08/2013	19°42′ 20.9″	96°43′ 39.9″	1,450	C/I
V15	Spring	El Castillo	Quaternary Volcanics	04/23/2013	19°32′ 42.7″	96°52′ 13.7″	1,150	C/I, T/C, CFC, NG
V18	Spring	Loma de Rogel	Pliocene Ignimbrites	05/07/2013	19°33′ 01.7″	96°48′ 02.1″	809	C/I, T/C
V20	Spring	Pocitos Cumbre	Cretaceous Limestone	05/09/2013	19°23′ 06.8″	96°38′ 46.0″	310	C/I
V28	Spring	Balneario Carrizal	Cretaceous Limestone	04/24/2013	19°19′ 14.5″	96°37′ 44.7″	195	C/I, T/C, CFC,
V51	Spring	Tengonapa 24 de Junio	Pliocene/Pleistocene Andesite-Andesite Tuff	04/25/2013	19°39′ 53.3″	96°59′ 24.5″	1,688	C/I, T/C, CFC, NG
V52	Spring	El Encinal	Quaternary Volcanics	05/06/2013	19°35′ 13.2″	97°03′ 58.5″	2,613	C/I
V53	Spring	El Arellano	Pliocene/Pleistocene Andesite-Andesite Tuff	05/10/2013	19°41′ 53.2″	96°59′ 36.1″	2,213	C/I
V55	Spring	Vaquerías I	Quaternary Volcanics	05/14/2013	19°28′ 04.6″	96°49′ 04.7″	978	C/I
V56	Spring	Tangerina	Quaternary Volcanics	05/11/2013	19°34′ 40.7″	96°54′ 58.7″	1,439	C/I
V19	Well	Dos Ríos	Pliocene Ignimbrites	04/23/2013	19°29′ 08.2″	96°48′ 06.4″	980	C/I, T/C, CFC
V33	Well	Espanata Judíos	Quaternary Alluvial	04/24/2013	19°29′ 01.4″	96°27′ 58.6″	71	C/I, T/C
V36	Well	San Rafael	Quaternary Alluvial	04/24/2013	19°24′ 52.0″	96°20′ 23.6″	10	C/I, T/C, CFC, NG
V37	Well	Cardel 1	Quaternary Alluvial	04/24/2013	19°22′ 01.9″	96°20′ 19.7″	10	C/I, T/C
V54	Well	Buena Vista	Cretaceous Limestone	05/13/2013	19°22′ 59.4″	96°34′ 32.9″	274	C/I, T/C

located in the headwaters of smaller catchments, contributing to the formation of perennial stream flow. The predominant groundwater flow direction in the Quaternary alluvial aquifer near the coast is from west to east, as shown by the potentiometric contours of Fig. 2. These contours are based on water-level data provided by the Comisión Nacional del Agua.

Methods

Hydrochemical and stable isotope contents were determined from a number of samples collected from springs, wells, rivers and sea water as part of an initial reconnaissance study during 2012. Based on the results of the previous study, 15 springs

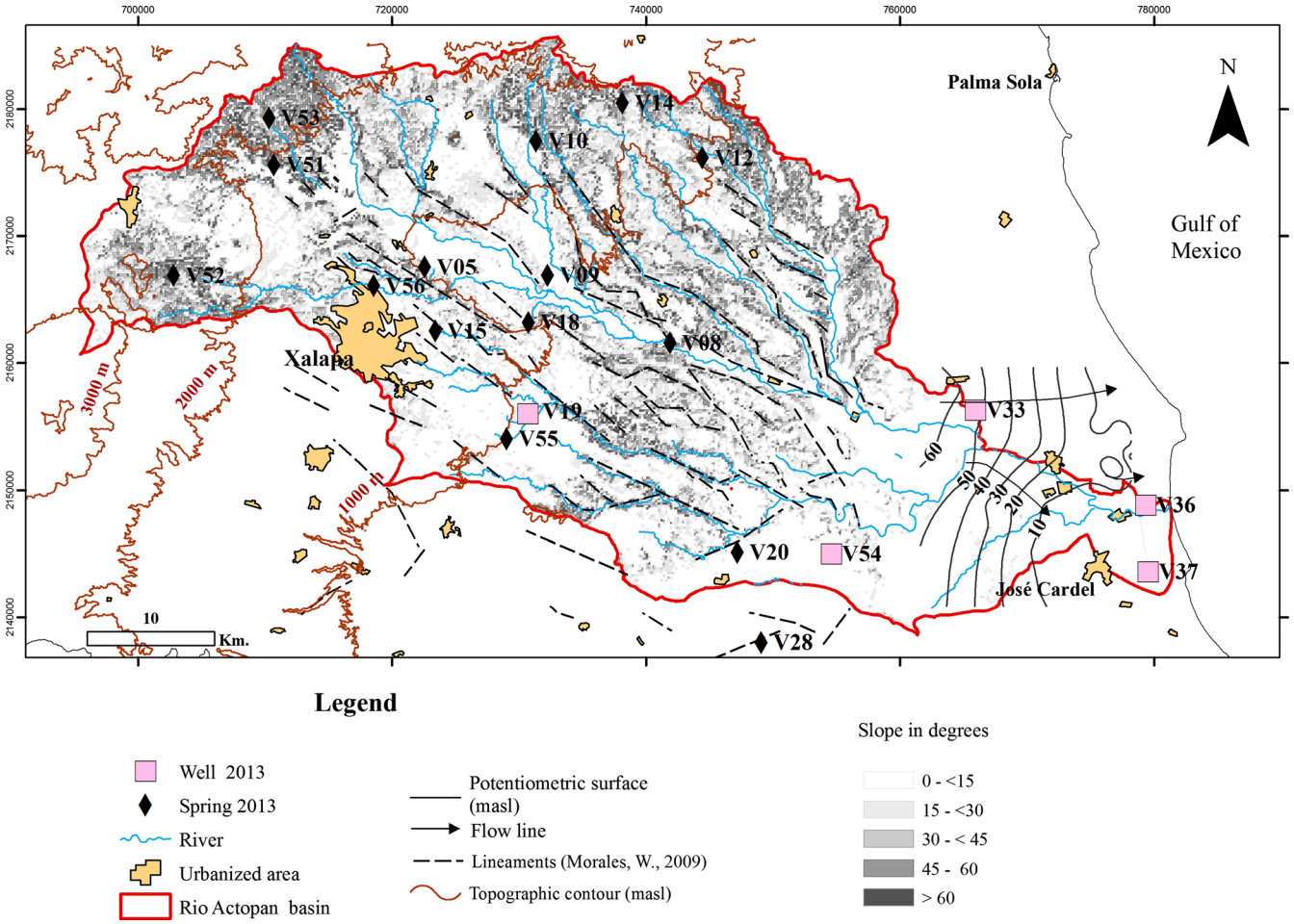

Fig. 2 Spatial relationship observed between major tectonic structures (lineaments) and the location of springs and wells in the Río Actopan Basin. The location of springs is partly controlled by the presence of these lineaments and locally steep topographic slopes (>30°). Hydraulic groundwater-level contours near the coast show the predominant west–east direction of groundwater flow, controlled by both the general topography gradient and well production near José Cardel. Modified from Morales-Barrera (2009)

and 5 wells were selected for hydrochemistry and stable isotopes (Table 1). From this group, a subset of seven springs and five wells were selected for analysis of tritium (^{3}H), carbon-14 (^{14}C) and carbon-13 (^{13}C), and a subset of five springs and two wells were selected for chlorofluorocarbon (CFC) analysis (CFC-11, CFC-12, CFC-113 and noble gases (He, Ne, Ar, Kr, Xe), but the noble-gas samples from three sites were contaminated. The selection criterion was based on sampling groundwater discharging from different hydrogeological units. In addition, 14 precipitation samples were collected during 2007 and 2008 for ^{3}H analysis.

Water samples were directly collected from the springs and wells at the first access point (before the addition of chlorine). These waters are commonly used for domestic supply and agricultural uses; the wells are typically pumped on a daily basis. Although the springs are perennial, the flow rate usually decreases up to 50 % during the dry season. Peristaltic pumps were used for the collection of spring samples. Samples for cation analyses were filtered using 0.45-μm filters and acidified with concentrated HNO_3. Temperature, pH, alkalinity and electrical conductivity were measured at all sampling points using standard field methods.

Chemical analyses were carried out at the Laboratorio de Química Ambiental, Universidad Nacional Autónoma de Mexico (UNAM), by ICP-OES for cations and ion chromatography for anions. $\delta^{18}O$ and $\delta^{2}H$ isotopic ratios, expressed as per mil deviations versus VSMOW, were determined at the Laboratorio de Espectrometría de Isótopos Estables del Instituto de Geología, UNAM, using a Gas Bench II coupled to a mass spectrometer stable isotope Thermo Finnigan MAT 253. Final $\delta^{18}O$ and $\delta^{2}H$ results were obtained after normalization in the VSMOW- SLAP scale, following the procedure outlined by Coplen (1988) and Wegner and Brand (2001). Radiocarbon and $\delta^{13}C$ analyses of total dissolved inorganic carbon (TDIC) were carried out at the Groningen University, Centre for Isotope Research (The Netherlands), by accelerator mass spectrometry (AMS). Measurement accuracy by AMS is typically in the range of 0.2–0.5 percent modern carbon

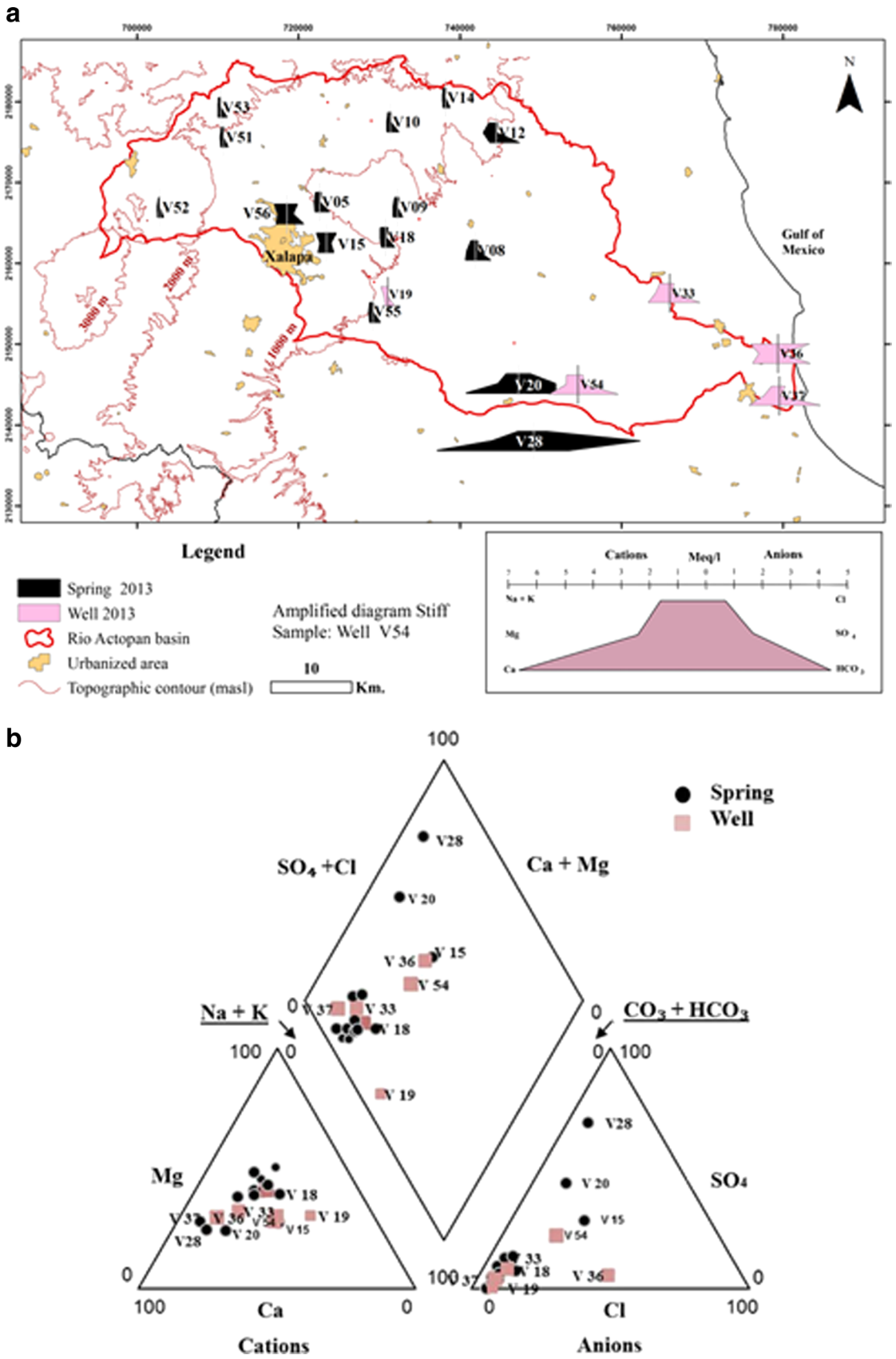

Fig. 3 **a** Map showing the spatial distribution of the hydrochemcial facies of groundwater in the Rio Actopan Basin using Stiff diagrams. **b** Piper diagram for the samples collected in 2013

(pmC) for ^{14}C and about ±1.0 ‰ for $\delta^{13}C$. Tritium analyses were carried out by HYDROSYS, Hungary, and the Isotope Hydrology Laboratory of the International Atomic Energy Agency (IHL-IAEA), Vienna (Austria), using electrolytic enrichment and a low-level liquid scintillation analyser, with a detection limit of 0.1 tritium units (TU) and uncertainty of ± 0.1–0.2 TU.

Analysis of dissolved noble gases from water samples was done at IHL-IAEA using dedicated static mass spectrometers for the determination of noble gas concentration and isotope abundances of noble gases dissolved in groundwater samples. Samples were collected in the field using standard 80-cm long × 1-cm diameter copper tube samplers. CFCs were collected in specifically designed brown glass bottles and also analyzed at IHL-IAEA in triplicate samples by a dedicated gas chromatographic system.

Results

Field parameters and major-ion chemistry

Table S1 of the electronic supplementary material (ESM) summarizes the results of field parameters and major-ion chemistry from samples collected from wells and springs in April and May 2013. Water temperature in springs ranged from 13 to 38 °C. The coolest temperature was measured in Spring V52, located at an elevation of 2,613 masl. The warmest temperature was measured in the thermal spring V28, located at 200 masl, indicating the existence of deep groundwater circulation. Most wells in the coastal plain had temperatures ranging from 23 to 30 °C, similar to the long-term mean annual air temperature in the area. Five hydrogeochemical samples have charge balances above 10 % which could be due to (1) analytical errors in the concentration determination or (2) ionic species having significant concentration levels that were not included in the analysis (Freeze and Cherry 1979).

The lowest specific conductance (SC) values are found in springs located at higher elevations (e.g. 52 μS/cm at V52) and the highest value (1,550 μS/cm) is from the thermal spring V28 closer to the coast, likely indicative of the degree of rock/water interaction due to varying flowpaths and geology. SC in the wells in the coastal plain ranges from 142 μS/cm in V19 located 10 km southeast of Xalapa to 890 μS/cm in V36, located at a short distance from the Actopan River and the coast. A similar trend is observed with chloride, ranging from less than 2 mg/L at high-elevation springs such as V51, V52, and V53 to 51 mg/L at V28. Cl concentrations in wells range from 2.6 mg/L in V19 (southeast of Xalapa) to 138 mg/L in V36 (along the coast). Nitrate concentrations in water from most wells and springs are below the 10 mg/L drinking-water standard, but two springs (V15 and V54) and one well (V37) exceed this with concentrations up to 44 mg/L; all three locations are near or downgradient of urban centers.

Piper and Stiff diagrams (Fig. 3) show that most groundwaters are classified as bicarbonate type (Na, K, Mg, or Ca), except thermal spring V28, which can be classified as calcium-sulfate type, and well V36, which has a sodium-chloride component. Spring V28 emanates from an outcropping limestone formation, but likely represents discharge from the deep regional groundwater flow based on its high temperature and sulphate concentration (700 mg/L). Well V36, located near the coast, seems to be a mixture of both calcium-bicarbonate and sodium-chloride types, perhaps indicating saltwater intrusion.

Stable isotopes

Stable-isotope analyses of springs and wells sampled in 2013 indicate a meteoric source of groundwater within the Rio Actopan Basin. Figure 4b ($\delta^{18}O$ versus $\delta^{2}H$) illustrates that these samples plot along both the global meteoric water line (GMWL), $\delta^{2}H = 8\ \delta^{18}O + 10$ (Craig 1961) and the local meteoric water line (LMWL), $\delta^{2}H = 7.44\ \delta^{18}O + 7.3$ (Pérez Quezadas et al. 2015). The $\delta^{18}O$ values of the 15 springs range from −7.1 to −9.6 ‰; $\delta^{2}H$ values range from −45.3 to −64.4 ‰ (Table S1 of the ESM). The isotopic values are more enriched for the five wells in the coastal plain, ranging from −5.5 to −7.3 ‰ for $\delta^{18}O$ and −36.5 to −48.5 ‰ for $\delta^{2}H$ (Table S1 of the ESM).

Figure 4 shows the relation between $\delta^{18}O$ and elevation of the site sampled, which is generally consistent with a previously published isotopic elevation gradient for precipitation in the Rio Actopan Basin (Pérez Quezadas et al. 2015). All of the springs above 1,400 masl, however, are slightly enriched compared with precipitation. This indicates some preferential recharge of isotopically enriched precipitation that is characteristic of the drier winter months, perhaps because of reduced evapotranspiration during this cooler period. Conversely, many of the springs and wells at elevations below 1,200 masl are slightly depleted compared with precipitation; this may be explained by recharge to these sites occurring at higher elevations in the watershed.

Carbon-14

Measured ^{14}C from 12 springs and wells ranged from about 12 to 96 pmC; $\delta^{13}C$ ranged from −3 to −19 ‰ VPDB (Table S2 of the ESM). Figure 5 shows ^{14}C (along with tritium) at several springs and wells along a NW–SE cross-section. Typical values are greater than 80 pmC in the upper part of the basin (spring V51) and less than 20 pmC in the coastal plain (well V54 and spring V28, both located in limestone formations). The Fontes and Garnier (1979) model was used to calculate the age using both ^{14}C and $\delta^{13}C$. This is a hybrid

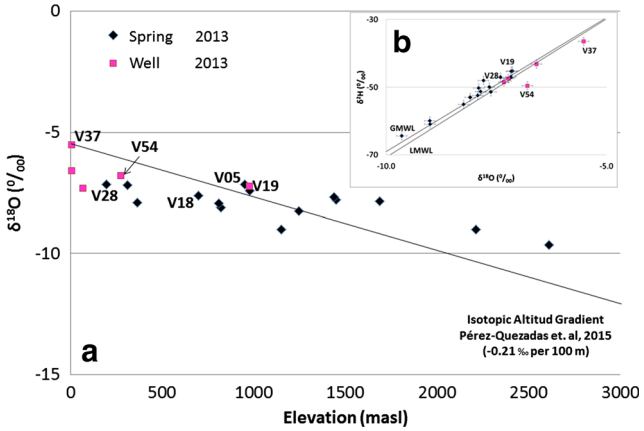

Fig. 4 **a** $\delta^{18}O$ contents of springs and wells in the Rio Actopan Basin compared to the isotopic elevation gradient of precipitation estimated by Pérez Quezadas et al. (2015). **b** The relationship between $\delta^{18}O$ and $\delta^{2}H$ values of spring and well samples and their position with respect to the global and local meteoric water lines (*GMWL*, *LMWL*, respectively)

of the Ingerson and Pearson (1964) model and Tamers (1975) model, combining both chemical and isotopic data to correct for exchange reaction effects on ^{14}C activity. It considers a two-stage evolution of recharge waters, using $\delta^{13}C$ to account for isotopic exchange with CO_2 in the unsaturated zone and isotopic exchange with carbonate rocks in the saturated zone. A chemical mass balance is performed similar to Tamers, with a provision for base exchange, to define the mass of carbon dissolved from inorganic sources (Plummer et al. 1994).

It is assumed that the corrected initial ^{14}C of infiltrating precipitation was 100 pmC (no bomb-pulse water) because measured values were less than or equal to 96 pmC, even for those having modern (post 1950s recharge) concentration of other environment tracers. Regarding isotopic exchange in the saturated zone, no published information was available for $\delta^{13}C$ of aquifer carbonates within the study area. A range of values from −2.0 to +2.0 % was tested, with values of +1.5 ‰ producing ^{14}C corrected ages most consistent with high tritium concentration (>0.5 TU) and the presence of CFCs at four springs (V15, V09, V51, and V08). For isotopic exchange in the vadose zone, soil zone $\delta^{13}C_{co2}$ was estimated by assuming that the predominant natural vegetation in the upland areas contributing to all of the springs and two higher elevation wells (V54 and V19) is primarily C3 plants (respiring more isotopically depleted $\delta^{13}C_{CO2}$, with end-member values ranging from about −17 to −30 ‰). The $\delta^{13}C_{co2}$ of the four young springs was individually adjusted within a range of about −17 to −30 ‰ until the corrected ^{14}C ages were modern (less than 100 years). Then the average $\delta^{13}C$ value for these four sites (−19.4 ‰) was used for three other springs (V28, V05, V18) and the two higher elevation wells (V19, V54), which all have low tritium (<0.3 TU). Similar to the group of springs with modern water, the group of lower elevation wells (V33, V36 and V37) all have high tritium (>0.5 TU) and, therefore, individual $\delta^{13}C$ values for each site were determined so that the corrected ^{14}C ages were modern (less than 100 years). The resulting "calibrated" $\delta^{13}C$ values were less depleted for these three wells (−11.7 to −15.7 ‰), consistent with the dominance of C4 plants ($\delta^{13}C_{CO2}$ of −10 to −16 ‰) such as sugar cane in agricultural areas in the lower part of the watershed. With these assumptions, corrected piston-flow ^{14}C ages of the three springs and two wells with low tritium (<0.3 TU) are all Holocene (about 5,000 years for spring V28, about 3,000 years for spring V05; about 500 years for spring V18; about 11,000 years for well V19; and about 7,000 years for well V54).

Tritium

Measured ^{3}H from 12 springs and wells ranged from about 0 to 1.9 TU (Table S2 of the ESM; Fig. 5). ^{3}H from precipitation samples collected in 2007 and 2008 ranged from 1.4 to 2.5 TU, with a mean value of 1.8 TU ($n = 14$). Comparison of groundwater concentration with corrected ^{14}C age (Fig. 6) shows that the ^{3}H results are consistent with ^{14}C results, with two distinct groups: (1) older waters having ^{14}C ages of about 3,000–11,000 years (sites V05, V19, V28, V54) with ^{3}H values of less than 0.3 TU; and (2) younger waters having ^{14}C ages of 30–500 years (sites V08, V09, V15, V18, V33, V36, V37, V51) with ^{3}H values of 1.9–0.5 TU.

Noble gases

Noble gas concentrations from three springs and one well (Table S3 of the ESM) were analyzed to evaluate recharge conditions, estimate excess air, and for dating

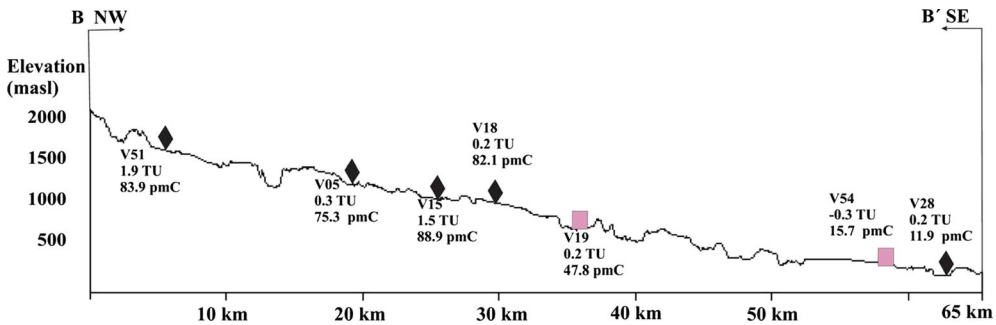

Fig. 5 Cross section along a NW–SE line showing the tritium and radiocarbon activities, expressed as tritium units (*TU*) and pmC, respectively. See Fig. 1 for location of the cross-section

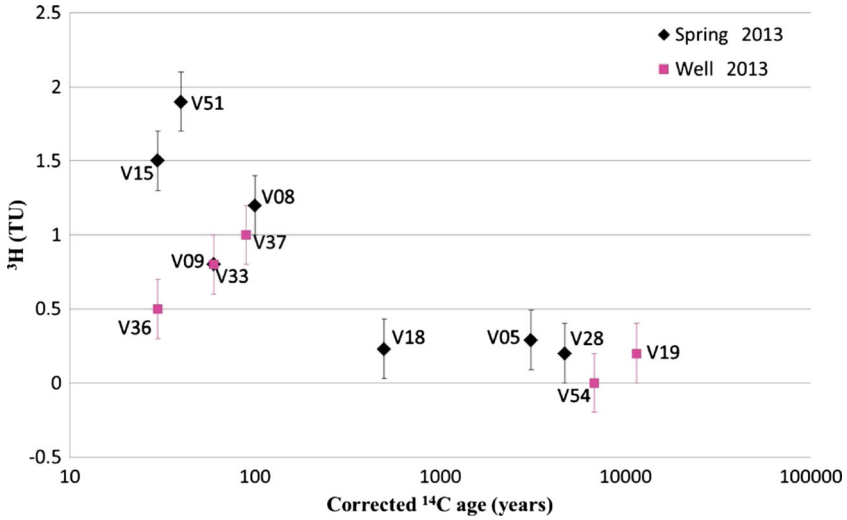

Fig. 6 ^{3}H compared with corrected ^{14}C age (log scale) for groundwater sites in the Río Actopan Basin. Maximum analytical uncertainty in the tritium activity is ± 0.2 TU

using the tritium/helium method ($^{3}H/^{3}He$) and terrigenic helium production ($^{4}He_{terr}$). Both the unfractionated air (UA; Stute and Schlosser 2000) and closed equilibrium (CE; Aeschbach-Hertig et al. 1999) models were used to fit concentrations of Ne, Ar, Kr, and Xe to theoretical values. These models evaluate recharge temperature governed by Henry's Law solubility (plus excess air) of dissolved gases entering the water table in the recharge zone using the χ^2 goodness of fit test with the excel-based "CalcAge" program (provided by Dr. Kip Solomon of the University of Utah, USA). Results of the simpler UA model are reported for this study because it produced good fits of less than a χ^2 probability threshold ($P < 5$ %) of 6.0 based on 2 degrees of freedom assuming four measured gases and the two parameters of recharge temperature and excess air.

While stable isotopes ($\delta^{18}O$, $\delta^{2}H$) indicate the source elevation of precipitation, they are unable to differentiate between recharge occurring at higher elevation versus surface-water runoff and recharge at lower elevation. Because the solubilities of noble gases are temperature-dependent, they can record the water temperature at which infiltration enters the aquifer, providing additional information on the elevation of the recharge zone. Because of the co-dependence of recharge elevation and recharge temperature, noble-gas recharge temperatures were calculated for both the elevation of sampling site (T_{Rmax}) and the maximum possible elevation of the water table within the watershed of 2,500 masl (T_{Rmin}). The maximum water-table elevation is based on the elevation of the highest springs within the watershed. The most-probable recharge elevation for each site was then determined as the intersection of the (T_{Rmin})/(T_{Rmax}) line with the groundwater temperature lapse rate (Manning and Solomon 2003). Recharge temperatures ranged from about 11–20 °C (Fig. 7; Table S3 of the ESM). These recharge temperatures are consistent with high-elevation (>1,100 m) recharge. Also, excess neon (ΔNe), an indicator of trapped air caused by water-table fluctuations in the recharge zone, ranged from 0 to about 30 %, indicating small to moderate amounts of additional gas dissolution during recharge.

The groundwater temperature lapse rate (about 6 °C per km) in this study is higher than one previously reported based on spring temperatures in the Wasatch Mountains of Utah, USA (Manning and Solomon 2003) but lower than those reported for other tropical areas, including the Cape Verde Islands, West Africa (Heilweil et al. 2012); it is within the range of atmospheric temperature lapse rates for the Cascade Mountains of Washington, USA (Minder et al. 2010). While groundwater lapse rates measured from springs do not account for the conversion of gravitational potential energy to heat through viscous dissipation of about 2 °C per km (Manga and Kirchner 2004), the lapse rate for the Rio Actopan watershed is consistent with the mean annual air temperature at the port of Veracruz of about 25.6 °C (Hernández López 2012).

$^{3}H/^{3}He_{trit}$ and $^{4}He_{ter}$

The noble gas analyses also provided measurements of total helium (He) and helium isotope ratios ($^{3}He/^{4}He$; Table S3 of the ESM). Using the equilibrium (plus excess air) solubility of the noble gases (Ne, Ar, Kr, Xe), along with measured He and $^{3}He/^{4}He$ ratio, terrigenic helium ($^{4}He_{ter}$) was calculated using "CalcAge" for the four sites with noble-gas data. $^{4}He_{ter}$ accumulation occurs with time as ^{4}He is produced as a byproduct of uranium and thorium decay in the aquifer matrix. Although this is only a qualitative indicator of groundwater ages between 10^{3} and 10^{6} years, older groundwater in an aquifer having uniform ^{4}He production rates would typically have higher $^{4}He_{ter}$ than younger groundwater (Solomon 2000). Calculations made for this study assume a terrigenic $^{3}He/^{4}He$ ratio of 2.8×10^{-8}, a value commonly used for crustal helium production during U/Th decay (Solomon 2000). While the

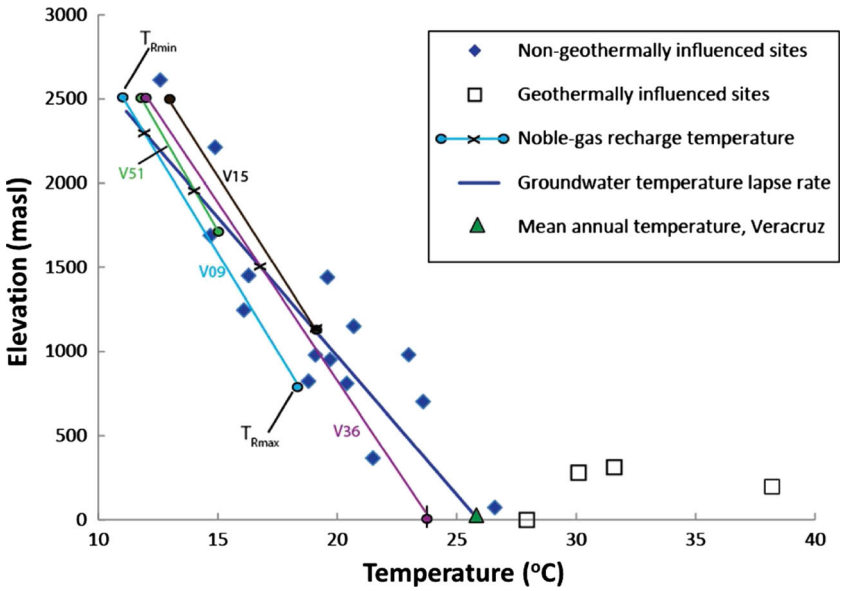

Fig. 7 Comparison of elevation to measured spring temperatures and calculated noble-gas recharge temperatures (T_R). The groundwater temperature lapse rate was calculated from measured spring temperatures for the sites not influenced by warm geothermal circulation. The most probable T_R is the interaction of the groundwater temperature lapse and the line between T_{Rmin} and T_{Rmax} for each site

actual ratio may be lower in the Río Actopan study area because of volcanism, there are no published data to support this. Using $^3He/^4He$ ratio of 2.8×10^{-8}, $^4He_{ter}$ concentrations at the four sites ranged from 6.7×10^{-11} to 4.9×10^{-9} ccSTP/g (Table S3 of the ESM), relatively small values that would be even less if a larger $^3He/^4He$ ratio were used. The lower two values from V09 and V51 (2.2×10^{-10} and 6.7×10^{-11} cc(STP)/g, respectively) are insignificant (essentially zero). All four sites are assumed to contain primarily young water based on their corrected ^{14}C ages of only 30 to 60 years. Sites having older ^{14}C ages in the Rio Actopan Basin such as at V19, V28, and V54, may contain higher amounts of terrigenic helium, but were not sampled for noble gases during this study.

Chlorofluorocarbons

Using the estimated recharge temperature, elevation, and excess air calculated from noble gases, measured chlorofluorocarbon (CFC) concentrations were converted to equivalent atmospheric concentrations (pptv) for age determination using the US Geological Survey (USGS) Reston Groundwater Dating Lab's CFC age calculator (Excel). The excess air used for four sites with noble gases (V09, V15, V36, V51) ranged from 0.02 to 2.6 cc/kg. The average value of 1 cc/kg was used for the other three sites without noble gases (V08, V19, V28). Calculated piston-flow ages were not very sensitive to the amount of excess air. For example, at the three sites without noble-gas derived excess air, an order of magnitude increase (to 10 cc/kg) changed the age by less than 0.5 years. Piston-flow years range from pre-1950s to the late 1980s (Table S2 of the ESM). The tracer-tracer plot of CFC-12 versus CFC-113 (Fig. 8) confirms piston-flow recharge conditions for springs V08 and V09, which were likely recharged in the late 1980s. Slightly older piston-flow ages for V08 and V09 determined from CFC-11, and for V15 determined from CFC-113 may be due to preferential bacterial anaerobic sulfate-reducing biodegradation of CFC-11 and CFC-113 (Plummer and Busenberg 2000). The tracer-tracer plot indicates that well V36 and spring V051 contain mixtures of young and older water. Assuming a binary mixing model, V36 contains about 25 % modern water recharged between 1985 and 1995 and 75 % recharge occurring more than 50 years ago. V51 contains about 80 % recent recharge (2013) and 20 % recharge occurring more than 50 years old. Young corrected ^{14}C ages for both V36 and V51 (Table S2 of the ESM) indicates that the "old" groundwater component at these sites is less than hundreds of years old. The tracer-tracer plot shows that both V19 and V28 have primarily pre-modern water. This is consistent with older ^{14}C ages (about 12,000 and 5,000 years, respectively) and low tritium (0.2 TU) for these sites.

Discussion: comparison of $^3H/^3He$ and CFC ages

For the sites such as V36 and V51 containing binary mixtures of younger and older groundwater, the $^3H/^3He$ age should theoretically be similar to the age of the young component determined by CFCs and younger than the CFC piston-flow age. This is because the $^3H/^3He$ age is determined by the amount of parent (^3H) relative to its daughter (^3He), the product of radioactive decay. This ratio remains unchanged even when diluted by older tritium-free water. In contrast, an "apparent" piston-flow CFC age would get older when diluted by older CFC-free water. This is true for spring V51, with a $^3H/^3He$ age of 4–2 ± 0.5 years and young component of the binary CFC12/113 mixing model recharged within 1 year of sampling, compared with piston-flow CFC ages of 25–28 years. But this is not true for well V36, which has a $^3H/^3He$ age of 39 years (recharge in 1974) which is similar

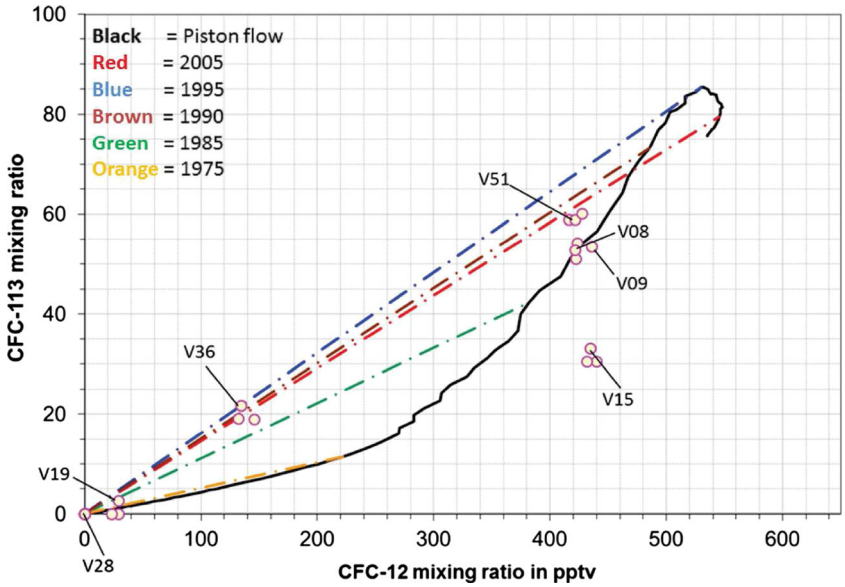

Fig. 8 Comparison of CFC-12 and CFC-113 equivalent atmospheric concentrations for groundwater in the Rio Actopan Basin, Veracruz, Mexico

to the piston-flow CFC age of 33–42 years, yet older than the young component age of 18–28 years for the binary mix based on CFC-12 and CFC-113. It is likely, therefore, that some tritiogenic ^{3}He was lost, either due to degassing at the spring orifice or during the sampling process. Such gas loss may also explain the discrepancies for springs V09 and V15, both having piston-flow recharge rather than binary mixtures with younger $^{3}H/^{3}He$ ages (10 and 4 years, respectively) than the piston-flow CFC-12 ages (mid-1980s recharge).

Conclusions

In order to better understand groundwater resources and groundwater quality within the Rio Actopan Basin, samples from 20 sites were collected for major-ion chemistry and stable isotopes. Carbon-14, tritium, chlorofluorocarbons, and noble gases were analyzed at selected sub-groups of these sites. Major-ion chemistry indicates that both salinity and water temperature generally increases in the lower part of the basin. Total dissolved solids in springs ranged from < 40 mg/L in the upper part of the watershed to >1,000 mg/L near the coast. Assuming most recharge occurs in the upper part of the basin, this increase likely indicates increased rock/water interaction associated with longer groundwater flowpaths. The geology within the basin (a mixture of volcanics, carbonates, and unconsolidated alluvial deposits) also controls the chemical signature of groundwater, resulting in calcium-bicarbonate, calcium-sulfate, and sodium-bicarbonate type waters. One well located near the coast has a mixture of both calcium-bicarbonate and sodium-chloride types, perhaps indicating some saltwater intrusion. Also, while most wells and springs have nitrate concentrations below the 10 mg/L drinking-water standard, two springs and one well near or downgradient of urban centers have concentrations between 20–44 mg/L.

Stable isotopes plot along a local meteoric water line previously defined by rainwater samples, indicating that recharge comes from precipitation falling at various elevations within the basin. All of the springs above 1,400 masl are slightly enriched compared with precipitation, indicating preferential recharge during the drier winter months. Many sites below 1,200 masl are slightly isotopically depleted, indicating their recharge occurs at higher elevations in the watershed. This is supported by cooler noble-gas recharge temperatures, which indicate that most of the recharge to the groundwater system occurs in the higher-elevation upland part of the basin.

The ages of groundwater in the Río Actopan Basin generally are Holocene to modern, indicating active groundwater recharge and relatively rapid movement through permeable aquifers. The wide range in ages (1 to >10,000 years) determined from environmental tracers indicates a variety of groundwater flowpaths and travel times within the watershed. While mixtures containing such old groundwater are unexpected in such a wet tropical setting, similar mixtures containing old groundwater (>1,000 years) were found in a tropical lowland rain forest in Costa Rica (Solomon et al. 2010).

Groundwater ages in the Río Actopan Basin derived from different tracers were generally consistent. For example, all the groundwater older than about 500 years based on ^{14}C has low tritium (<0.5 TU), whereas all of the younger groundwater has tritium between 0.5 and 2 TU. Similarly, ages determined with $^{3}H/^{3}He$ are generally consistent with piston-flow CFC ages, but because the sampling sites included both springs and production wells with long screened intervals (rather than monitoring wells with short screen intervals), some groundwater samples are mixtures of two or more flow paths. This is supported by a CFC-12 versus CFC-113 tracer-

tracer plot, with some samples located along a piston-flow line, while others are along binary mixing lines of young and older groundwater. In conclusion, the data collection and interpretation confirmed the study's hypothesis that the groundwater system within the Rio Actopan Basin is relatively active, with the majority of recharge to the groundwater system occurring in the upland parts of the watershed and moving towards the coast.

Acknowledgements Authors are thankful to the Consejo de Ciencia y Tecnología, CONACyT, for the support provided to the first author of this study. Sincere thanks are due to the staff of the Stable Isotope Laboratory of the Geology Institute, Autonomous University of Mexico (Pedro Morales Puente and Edith Cienfuegos Alvarado) as well as the Hydrochemistry Laboratory at the Geosciences Centre, UNAM (Carolina Muños Torres). We also thank Dr. Kip Solomon for providing the Excel-based "CalcAge" software used for noble-gas recharge temperature, $^{3}H/^{3}He$ age, and $^{4}He_{terr}$ interpretations. We also thank the USGS Reston Groundwater Dating Laboratory for providing the Excel-based software used for chlorofluorocarbon dating. Part of this study was carried out as part of the Technical Cooperation Project MEX7010, supported by the International Atomic Energy Agency.

References

Aeschbach-Hertig W, Peeters F, Beyerle U, Kipfer R (1999) Interpretation of dissolved atmospheric noble gases in natural waters. Water Resour Res 35:2779–2792

Cook PG, Bohlke JK (2000) Determining timescales for groundwater flow and solute transport. In: Cook PG, Herczeg AL (eds) Environmental tracers in subsurface hydrology. Kluwer, Boston, pp 1–30

Comisión Nacional del Agua (CONAGUA) (2002) Actualización de la disponibilidad media anual de agua subterránea. Acuífero (3005) Valle de Actopan Estado de Veracruz México [Updating the annual average availability of groundwater. Aquifer (3005) Actopan Valley, State of Veracruz Mexico]. Gerencia de Aguas Subterráneas, CONAGUA, Mexico City

Coplen TB (1988) Normalization of oxygen and hydrogen isotope data, chemical geology. Isotope Geosci 72(4):293–297. doi:10.1016/0168-9622(88)90042-5

Craig H (1961) Isotopic variations in meteoric waters. Science 133(3465):1702–1703

Fontes JC, Garnier JM (1979) Determination of the initial ^{14}C activity of the total dissolved carbon: a review of the existing models and a new approach. Water Resour Res 15(2):399–413. doi:10.1029/WR015i002p00399

Freeze A, Cherry J (1979) Groundwater. Prentice-Hall, Upper Saddle River, NJ

Gardner PM, Heilweil VM (2014) A multiple-tracer approach to understanding regional groundwater flow in the Snake Valley area of eastern Great Basin, USA. Appl Geochem 45:33–49

Geo-Mexico (2014) Mexico's seven climatic regions, Geo-Mexico, the geography and dynamics of modern Mexico. http://geo-mexico.com/?p=9512. Accessed 8 December 2014

Goldsmith GR, Muños-Villers LE, Holwerda F, McDonnell JJ, Asbjornsen H, Dawson TE (2011) Stable isotopes reveal linkages among ecohydrological processes in a seasonally dry tropical montane cloud forest. Ecohydrology 5:779–790. doi:10.1002/eco.268

Gómez A (2002) Control temporal del magmatismo de subducción en la porción oriental de la Faja Volcánica Transmexicana: caracerización del manto, components en subducción y contaminación cortical [Temporary control of subduction magmatism in the eastern portion of the Mexican Volcanic Belt: characterization of mantle components in subduction and crustal contamination]. PhD Thesis, Instituto de Geología, UNAM, Mexico

Healy RW, Winter TC, Labaugh JW, Franke OL (2007) Water budgets: foundations for effective water-resources and environmental management. US Geol Surv Circ 1308

Heilweil VM, Healy RW, Harris RN (2012) Noble gases and coupled heat/fluid flow modeling for evaluating hydrogeologic conditions of volcanic island aquifers. J Hydrol 464–465:309–327

Heilweil VM, Sweetkind DS, Gerner SJ (2014) Innovative environmental tracer techniques for evaluating sources of spring discharge from a carbonate aquifer bisected by a river. Groundwater 52(1):71–83

Hernández López C (2012) Análisis del comportamiento de la temperatura y la precipitación mediante climogramas y tendencias en la zona central de Veracruz [Analysis of the behavior of temperature and precipitation by climograms and trends in central Veracruz]. BA Thesis, Universidad Veracruzana, Xalapa, Veracruz, Mexico

Ingerson E, Pearson FJ (1964) Estimation of age and rate of motion of groundwater by the ^{14}C-method. In: Miyake Y (ed) Recent researches in the field of hydrosphere, atmosphere and nuclear geochemistry. Nagoya, Maruzen, Tokyo, pp 263–283

Intenational Atomic Energy Agency (IAEA) (2013) Isotope methods for dating groundwater. IAEA, Vienna

Jones SC, Harr PA, Abraham J, Bosart LF, Bowyer PJ, Evans JL, Hanley DE, Hanstrum BN, Hart RE, Lalaurette F, Sinclair MR, Smith RK, Thorncroft C (2003) The extratropical transition of tropical cyclones: forecast challenges, current understanding and future directions. Weather Forecast 18(6):1052–1092. doi:10.1175/1520-0434(2003)018 1052:TETOTC 2.0.CO;2

López-Infanzón M (1991) Petrologic study of the volcanic rocks in the Chiconquiaco-Palma Sola. MSc Thesis, Tulane University, New Orleans, LA, USA

Manga M, Kirchner JW (2004) Interpreting the temperature of water at cold springs and the importance of gravitational potential energy. Water Resour Res 40(5). doi:10.1029/2003WR002905

Magaña V, Vazquez JL, Pérez JL, Pérez JV (2003) Impact of El Niño on precipitation in Mexico. Geof Int 42(3):313–330

Manning AH, Solomon DK (2003) Using noble gases to investigate mountain-front recharge. J Hydrol 275:194–207

Mantua NJ, Hare SR, Zhang Y, Wallace JM, Francis RC (1997) A Pacific decadal climate oscillation with impacts on salmon production. Bull Am Meteorol Soc 78:1069–1079

Méndez González J, Ramírez Leyva A, Cornejo Oviedo A, Zárate Lupercio A, Cabazos Pérez T (2010) Teleconexiones de la Oscilación Decadal del Pacífico (PDO) a la precipitación y temperatura en México [Teleconnections of Pacific Decadal Oscillation (PDO) to precipitation and temperature in Mexico] Invest Geográf 73:28–79

Minder JR, Mote PW, Lundquist JD (2010) Surface temperature lapse rates over complex terrain: lessons from the Cascade Mountains. J Geophys Res 115:D14122. doi:10.1029/2009JD013493

Morales-Barrera W (2009) Estudio geológico de un depósito ignimbrítico en la región de Xalapa, Veracruz: distribución, estratigrafía, petrografía y geoquímica [Geological survey of ignimbrite deposit in the region of Xalapa, Veracruz: distribution, stratigraphy, petrography and geochemistry]. MSc Thesis. Universidad Nacional Autónoma de México, Mexico

Mosiño P, García E (1973) The climate of Mexico. In: Bryson RA, Hare FK (eds) Climates of North America. Elsevier, Amsterdam, pp 345–404

Negendank JFW, Emmermann R, Krawczyk R, Mooser F, Tobschall H, Werle D (1985) Geological and geochemical investigations on the eastern Trans-Mexican Volcanic Belt. Geof Int 24(4):477–575

Newman BD, Osenbrück K, Aeschbach-Hertig W, Solomon DK, Cook P, Rózánski K, Kipfer R (2010) Dating of 'young' groundwaters using environmental tracers: Advantages, applications, and research needs. Isot Environ Health Stud 46(3):259–278

Pérez Quezadas J, Cortés Silva A, Inguaggiato S, Salas Ortega MR, Cervantes Pérez J, Heilweil VM (2015) Meteoric isotopic gradient on the windward side of the Sierra Madre Oriental area, Veracruz, México. Geof Int 54(3):267–276

Plummer LN, Busenberg E (2000) Chlorofluorocarbons. In: Cook PG, Herczeg AL (eds) Environmental tracers in subsurface hydrology. Kluwer, Boston, pp 441–478

Plummer LN, Michel RL, Thurman EM, Glynn PD (1993) Environmental tracers for age-dating young groundwater. In: Alley W (ed) Regional ground-water quality. Reinhold, New York, pp 255–294

Plummer LN, Prestemon EC, Parkhurst DL (1994) An interactive code (NETPATH) for modeling net geochemical reactions along a flow path version 2.0. US Geol Surv Water Resour Invest Rep 94-4169

Rasmusson EM, Wallace JM (1983) Meteorological aspects of the El Niño/Southern Oscillation. Science 222(4629):1195–1202

Rodríguez SR, Morales W, Layer P, González E (2010) A Quaternary monogenetic volcanic field in the Xalapa region, eastern Trans-Mexican Volcanic Belt: geology, distribution and morphology of the volcanic vents. J Volcanol Geotherm Res 197:146–166. doi:10.1016/j.jvolgeores.2009.08.003

Salas-Ortega R (2010) Estudio geológico e hidrogeoquímico de un sistema de manantiales en la región de Xalapa, Veracruz [Geological and hydro-geochemical study of a system of springs in the region of Xalapa, Veracruz]. MSc Thesis, Universidad Nacional Autónoma de México, Mexico

Santamaría-Orozco D, Arenas-Partida R, Escamilla-Herrera A (1990) Normalización de la Nomenclatura Estratigráfica en las Cuencas Mesozoicas de México [Stratigraphic nomenclature normalization of Mesozoic basins in Mexico]. Inst Mex Petróleo 19:102–106

Servicio Geológico Mexicano (SGM) (2007a) Carta Geológico-minera Xalapa E14-B27 Veracruz Escala 1:50 000 [Geological map Xalapa E14-B27 Veracuz Scale 1:50,000]. Consejo de Recursos Minerales, Pachuca, Hidalgo, Mexico

Servicio Geológico Mexicano (SGM) (2007b) Carta Geológico-minera Perote E14-B26 Veracruz Escala 1:50 000 [Geological map Perote E14-B26 Veracruz Scale 1:50,000]. Consejo de Recursos Minerales, Pachuca, Hidalgo, Mexico

Servicio Geológico Mexicano (SGM) (2010) Carta Geológico-minera Coatepec E14-B37 Veracruz-Puebla Escala 1:50 000 [Geological map Coatepec E14-B37 Veracruz-Puebla Scale 1:50,000]. Servicio Geológico Mexicano, Pachuca, Hidalgo, Mexico

Solomon DK (2000) ^{4}He in groundwater. In: Cook PG, Herczeg AL (eds) Environmental tracers in subsurface hydrology. Kluwer, Boston, pp 425–439

Solomon DK, Genereux DP, Plummer LN, Busenberg E (2010) Testing mixing models of old and young groundwater in a tropical lowland rain forest with environmental tracers. Water Resour Res 46. doi:10.1029/2009WR008341

Stute M, Schlosser P (2000) Atmospheric noble gases. In: Cook PG, Herczeg AL (eds) Environmental tracers in subsurface hydrology. Kluwer, Boston, pp 349–377

Sutton R, Hodson D (2005) Atlantic ocean forcing of North American and European summer climate. Science 309(5731):115–117. doi:10.1126/science.1109496

Tamers MA (1975) Validity of radiocarbon dates on groundwater. Geophys Surv 2(2):217–239. doi:10.1007/BF01447909

Tejeda A, Acevedo F, Jáuregui E (1989) Atlas Climático del Estado de Veracruz Colección Textos Universitarios [Climate Atlas of the state of Veracruz Texts university collection]. Universidad Veracruzana, Xalapa, Mexico

Vázquez JL (2007) Variabilidad de la precipitación en la República Mexicana [Variability of precipitation in the Mexican Republic]. PhD Thesis, Universidad Nacional Autónoma de México, Mexico

Viniegra-Osorio F (1965) Geología del Macizo de Teziutlán y la Cuenca Cenozoica de Veracruz y La Cuenca Cenozoica de Veracruz Papaloapan [Teziutlán Massif Geology and Cenozoic Basin Veracruz]. Bol Asoc Mexicana Geól Petrol 1:315–384

Wegner RA, Brand WA (2001) Referencing strategies and techniques in stable isotope radio analysis. Rapid Commun Mass Spectrom 15: 501–519. doi:10.1002/rcm.258

Yager RM, Plummer LN, Kauffman LJ, Doctor DH, Nelms DL, Schlosser P (2013) Comparison of age distributions estimated from environmental tracers by using binary-dilution and numerical models of fractured and folded karst: Shenandoah Valley of Virginia and West Virginia, USA. Hydrogeol J 21(6):1193–1217